

Modelling of tornado and microburst-induced wind loading and failure of a lattice transmission tower

Eric Savory^{*}, Gerard A.R. Parke, Mostafa Zeinoddini, Norman Toy, Peter Disney

Department of Civil Engineering, University of Surrey, Guildford, GU2 7XH, UK

Received 12 December 1998; received in revised form 17 April 2000; accepted 20 April 2000

Abstract

Many transmission line and tower failures worldwide are attributed to high intensity winds (HIW) associated with tornadoes and microbursts. This paper describes models for the wind velocity time–histories of transient tornado and microburst events and the resulting loading on a lattice tower. A dynamic structural analysis has been undertaken for two HIW events, predicting a tornado-induced shear failure, as observed in the field. However, the microburst does not produce failure, due to its lower intensity and longer duration. Indeed, such failures, if they occur in practice, are likely to be associated with a more broad-fronted microburst loading in which conductor loads contribute. © 2000 Elsevier Science Ltd. All rights reserved.

Keywords: Wind; Tower; Failure

1. Introduction

When designing transmission towers with conventional geometries and conductor arrangements the engineer has many design codes and guides available [1–5]. These design procedures consider the mean wind loads acting on the conductors and tower members and also take into account the quasi-steady dynamic loads induced by the conductors on the tower, as well as the effects of localised “patch” loads. Despite the availability of such codes our understanding of the behaviour of transmission lines remains incomplete [6]. In many cases the main cause of transmission tower failure is the loading arising under off-design conditions due to the actions of High Intensity Winds (HIW) [7]. Indeed, transmission tower failure due to the action of HIW is a major and costly problem in the Americas, Australasia and South Africa with many of the utility organisations reporting that 80–100% of all weather-related failures are the result of HIW. These meteorological phenomena are localised and unpredictable, such that their structure, scale and intensity cannot readily be measured in the

field by conventional recording stations. It is not always the high wind speed which causes tower failure but, rather, the fact that the localised wind structure may impose loads which are not normally taken into account in the design. Such HIW may be associated with various downbursts and microbursts, as well as mature tornadoes.

In a conventional design the engineer takes into account both the wind load on the tower and, more importantly, the weight of the transmission conductors and the wind load on them. From these load sources, the line of action of the resultant transverse forces may be determined allowing the tower to be designed such that the internal face members act to brace the structure but do not take significant loads themselves. For normal wind conditions, even at high wind speeds, this arrangement is adequate. However, in the case of HIW in the form of tornadoes the wind structure may be so localised that only the tower is significantly affected and not the conductors. In addition, for all types of HIW the shape of the gust may further act to change the line of action of the wind loads, normally moving it closer to the ground level [7]. In this radically off-design condition tower failure may occur, sometimes initiated by collapse of the members in the windward faces of the tower. Since such behaviour is not accounted for within current conventional design processes it is imperative that new

^{*} Corresponding author. Tel.: +44-1483-876631; fax: +44-1483-450984.

E-mail address: e.savory@surrey.ac.uk (E. Savory).

methodologies are adopted, both for remedial action on existing towers and for HIW-resistant design of new lines.

Hence, a more rational design of transmission line systems in those parts of the world where HIW are a common occurrence needs to include assessments of tower or conductor failure due to the effects of those winds. Models are being developed, based upon evidence of HIW occurrence and damage, in which statistical analyses of the data are used to assess the probability of a HIW of a particular intensity and scale intercepting a specified length of line. In the case of tornadoes, general risk assessment models have been developed [8,9], whilst others have been formulated for specific countries such as South Africa [10] and Argentina [11]. Risk assessment models for downbursts have been proposed by a number of workers [12–14], the latter focusing upon Australia. However, it has recently been noted [15] that the actual physical characteristics of HIW events, together with our ability to model them, have been a largely neglected area of wind engineering research.

Related to the issue of risk is the question of what then happens when a HIW impacts upon a transmission line? What are the time–histories of the wind profiles as the event passes the line and what are the associated loading distributions? How do these loading histories cause failure of the towers and what are the failure modes? Since HIW events are very localised and each is different in character there is little data available with which to make such assessments. Nevertheless, it should be possible to develop initially simple numerical models for HIW-induced transmission line loading time–histories. The data generated may then be utilised as the input to finite element structural analysis models. By applying these type of loading profiles to such analysis models, with increasing refinement, it may be possible to predict the failure modes which are observed in the field and, thereby, gain a greater understanding of the manner in which such winds interact with the tower. The work presented in this paper is intended to contribute towards such developments.

Before discussing the wind profile models it is necessary to note that the flow field associated with a tornado is very different from that associated with a microburst. Hence, even though the two events may be similar in intensity and may have the potential to cause failure of a transmission tower the actual failure modes would probably be different. Tornadoes that extend to the ground are characterised by strong vortical motion in the horizontal plane, perhaps with secondary suction vortices, and these motions are convected laterally by the local environmental wind field [16]. In contrast, downbursts of different scales, including microbursts, are characterised by a “wall jet” which rapidly spreads radially outwards after touch down and may, again, be convected by the ambient wind field. The basic form of

microbursts has been described [17], from observational evidence, as being a rapid and intense downburst of air, forming a vortex ring with a horizontal extent of less than 4 km, which makes contact with the ground and spreads quickly outwards. This entire process occurs within about 2 minutes and, after ground contact, the highest lateral wind speeds are directly beneath the ring vortex core, typically 30–100 m above ground level. Although downbursts may possess some rotation in the horizontal plane [18], the magnitude of the induced rotational wind velocities, typically of the order of 2 m/s, would be insignificant in terms of any transmission tower loadings.

2. The tornado model

The tornado wind field and loading model utilised here is that conveniently presented by earlier authors [8,19] and the reader is referred to those texts for a full listing of the relevant equations. However, Fig. 1 shows the basic structure of the modelled tornado for which the equations give the three components of velocity (tangential, radial and vertical) and their temporal and spatial variations during the event. The model then uses this data to predict the loading on an obstacle in the path of a tornado, taking into account both the static drag forces and the inertia forces due to the accelerations in the wind flow as the event passes the site. Hence, the overall force per unit height of the obstacle at any given time, $F(t)$, may be given by

$$F(t) = \frac{1}{2} \rho C_d D U |U| + \frac{\pi}{4} \rho C_m D^2 \frac{dU}{dt}$$

where C_d and C_m are the drag and inertia coefficients, respectively, ρ is the air density, U is the velocity component in the direction being considered and D is

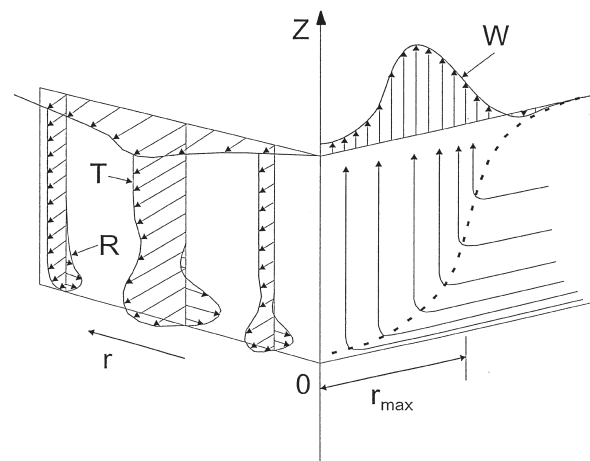


Fig. 1. Basic wind field structure of the modelled tornado [8,19] (R =radial velocity component, T =tangential velocity component, W =vertical velocity component).

the projected width of the obstacle normal to that direction. The model is very flexible in that it takes into account the offset of the obstacle from the path of the tornado and the angle of the front face of the obstacle (in this case the line of the transmission conductors) to that path. The velocity vectors, velocity gradients and accelerations are resolved to give the horizontal velocity components normal to the front face of the obstacle, or normal to the transmission line (U in the x -direction), and at right angles to this direction (V in the y -direction). Hence, the forcing time histories in those two directions, F_x and F_y , may be computed for application to the structural analysis model.

3. The microburst model

There are essentially two forms of simplified models for the wind field associated with a downburst, namely the “ring vortex” model [20–22] and the impinging wall jet model [22,24]. These two approaches are illustrated schematically in Fig. 2. The first type of model has arisen because of the manner in which the descending column of air forms a vortex ring prior to touching the ground. However, after touch down it is the radial outflow in the form of a wall jet which dominates the wind field, such that wall jet models have been found to provide the better representation of the fully-developed microburst. Indeed, recent attempts to simulate scaled microburst events in a laboratory using a large impinging jet have shown good agreement with some of the available full-scale data [25,26].

The nature of the loading imposed on a transmission tower by a microburst will depend upon the stage of the development of the event when it interacts with the tower. If the downburst is close to the ground and approaching touch down then there may well be a significant vertical loading component on the tower. This may act upwards or downwards depending upon how the microburst vortex intersects the tower and so such loading patterns are very difficult to predict. However, if the microburst has already reached the ground and is spreading outward as it impinges upon the tower then the main loading components will be in the horizontal plane. It is this more straightforward case which is considered in the present paper, even though it is recognised that the maximum winds occur close to the touchdown point.

The model adopted here is that presented by previous workers [23,24] which permits the prediction of the variation of the horizontal wind speed vector with time as a microburst with initially defined characteristics passes a specified place, such as the location of a transmission tower. Here, the model is augmented to give wind profiles at different heights (Z) above the ground by using a vertical profile of horizontal radial mean wind velocity (U) of the form presented earlier in a wall jet model [22], namely

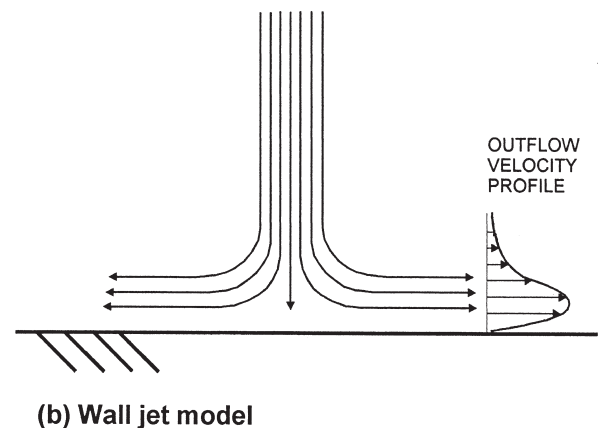
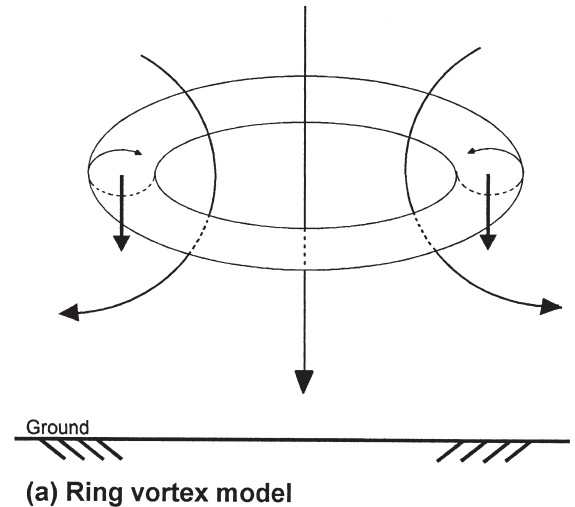


Fig. 2. Ring vortex and impinging wall jet models for a microburst.

$$\frac{U}{U_{\max}} = e^{(-0.15 \frac{Z}{Z_{\max}})} - e^{(-3.2175 \frac{Z}{Z_{\max}})}$$

where, at any given radial distance from the microburst centre, U_{\max} is the maximum horizontal radial velocity within the microburst which occurs at a height Z_{\max} above the ground (typically Z_{\max} is about 60 m). This profile is illustrated in Fig. 3.

In the present work, a modified form of the tornado loading model described earlier is utilised to give the microburst-induced loads. This is achieved by using the same basic equations for deriving the flow accelerations from the temporal and spatial variations of the wind velocity but with small modifications to allow the use of the microburst wind field data as the input. The same loading equations are then used to give the forcing time

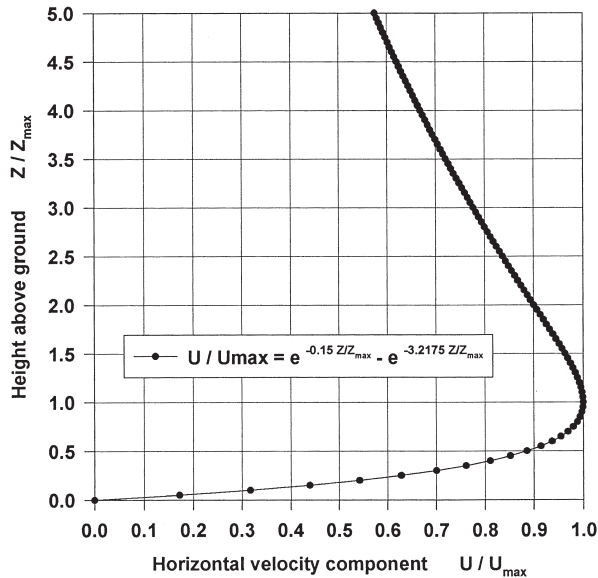


Fig. 3. Vertical profile of the horizontal radial outflow wind speed associated with a microburst.

histories from the horizontal velocity field. Since only a well-developed microburst is being considered here, as a wall-jet, the vertical component of the velocity and the temporal and spatial rates of change of that component are ignored. In both models only the large-scale motions associated with the HIW event are considered so that smaller-scale wind turbulence is neglected. Hence, the gust velocities are neglected such that the spatial and temporal rates of change are effectively mean windspeed gradients.

4. Details of the modelled tower

Before computing the wind fields and loading histories associated with microburst and tornado events it is important to assess how those loads may be transmitted to the tower. In the present work the tower chosen to illustrate the application of the model is a CEGB type Blaw Knox L6 standard height lattice tower [27], for which a structural analysis model using the finite element code ABAQUS [28] had, conveniently, previously been implemented [29]. As part of that research, the wind-induced foundation loads have also been monitored on a full-scale tower in the UK. Although such a tower is not normally located in regions of regular HIW occurrence, it is adopted here simply as a representation of a generic lattice tower.

The modelled tower, which has a height of 50.5 m and a square base area of 9.1×9.1 m, is illustrated in Fig. 4. The mean height of the conductors above ground level is 30 m and the typical effective conductor span is 341 m between adjacent towers along the line [29]. ABAQUS three-dimensional beam elements type B31

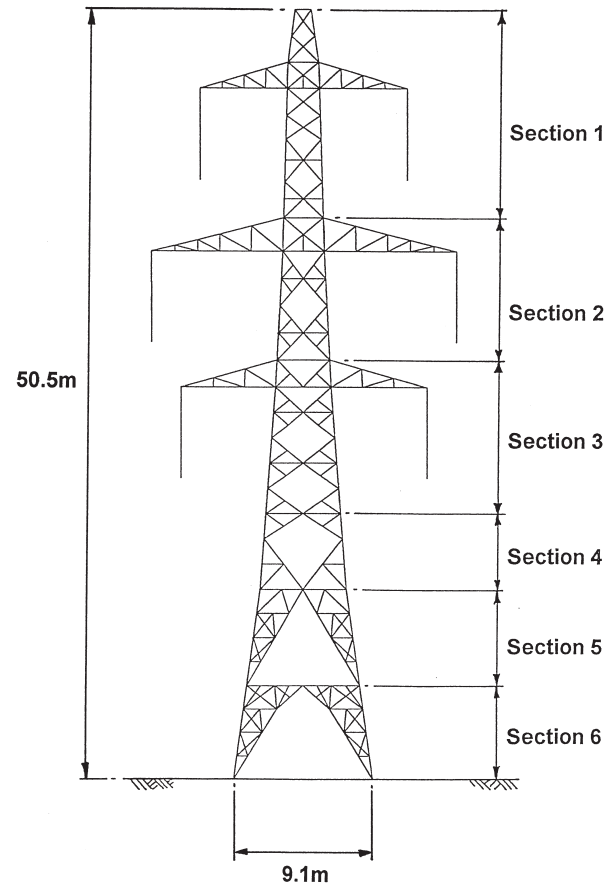


Fig. 4. Outline of the modelled lattice transmission tower.

have been employed to model the tower members. A relatively small value for the moment of inertia has been used for the beam elements in order to keep the bending and torsional stiffness at both ends of the members close to zero. This simulates almost pinned connections for the structural model that is close to the real connection response exhibited in the actual structure [30]. The cross-sectional areas of the modelled members are the same as the real members. By using a low bending stiffness and the true axial stiffness, the tower members are modelled as truss elements, the behaviour of which includes a full post-buckling response. The restraining influence of the transmission conductors has been included in the tower model and the self-weight of the conductors and tower are also incorporated in the analysis. However, strain hardening and the strain dependence in the material has not been considered for the beam elements.

The numerical model has been used to obtain the response of the tower to the tornado and microburst wind loads and to investigate the possibility of a dynamic failure in the structure. An implicit, incremental, direct integration approach has been used for this purpose, which allows modelling of the tower inertia forces. The direct

integration method is necessary to maintain numerical stability when non-linear responses are expected. With this method all of the equations of motion of the system are integrated through time. The results of the current time increment are used as the initial conditions for the solution of the equations of motion in the next time increment. Furthermore, when the structural system is dynamically sensitive and liable to large non-linearity or dynamic instability, very small time increments are required when running the program. For dynamically sensitive structures, such as the tower model (particularly under the tornado wind loading), a considerable amount of time is needed for each single analysis.

A small amount of mass damping has been incorporated into the numerical model. This does not appreciably affect the overall response of the model but serves to damp an initial vibration that occurs as a result of the application of a small step load at the start of the time history.

In this study the possibility of structural failure due to an extreme wind load has been investigated. With an implicit direct integration approach, if the response of a structure to a dynamic excitation is bounded it is considered that the excited structure remains stable and no failure occurs. An unbounded response indicates the propagation of dynamic instability in the system. For a multi-degree of freedom system an exact solution for the dynamic limit point load does not exist and so only minimum guaranteed critical loads can be evaluated.

In the present work, for computing the total wind load on the structure the solid area of each face of the lattice tower was determined and a drag coefficient of 3.0 applied to the area of one face. This is approximately the value specified in Fig. 4.3(a) of the UK Code of Practice for a lattice tower with a solidity ratio of 18% [31] and takes into account the shielding of the leeward members by the windward ones. If a sensible drag coefficient of 2.0 is taken for the typical right-angle members utilised in the tower [32:31], then the overall value applied indicates that the leeward members take about 1/3rd of the total load which would seem reasonable. The full computed load is applied to the tower, implying a gust factor of 1.0, as recommended by the ASCE guidelines concerning tornadic winds [5]. The choice of a value for the inertia coefficient is not obvious since it should be determined experimentally. However, previous work [19] suggests that a value close to unity is appropriate and, hence, in the present model an inertia coefficient of 1.0 is implemented. It is rather time-consuming and, hence, not very practical to directly compute the individual loads in each member of the tower from the loading time histories. Rather the tower is divided into six vertical sections, approximately equal in height as shown in Fig. 4, and the overall loadings on these “patches” computed in the longitudinal or x -direc-

tion (normal to the conductors) and the transverse or y -direction (parallel to the conductors and including the cross-arms of the tower).

Both the x and y components of the wind load have been used simultaneously in the dynamic analysis. The time history of the load has been introduced into the program using the AMPLITUDE option in ABAQUS. At every time increment the incident wind load at each section has been applied at the corner nodes of the horizontal plan bracing existing at that level, as illustrated in Fig. 5. Each front node receives 1/3rd of the load acting at that level and each back node 1/6th of the load. For these narrow-fronted HIW only the wind loading on the tower is included since typical HIW-induced damage of transmission lines indicates [7] that the contribution to the tower loads from the conductors is secondary under these conditions. Whilst this assumption is probably satisfactory when considering tornado loads, it is not strictly appropriate for the much larger-scale microburst events.

5. Details of the modelled tornado and microburst

Two events have been studied, namely one tornado and one microburst. Both have been deliberately chosen to be severe events, typically F3 on the Fujita scale [33], but, clearly, it is not possible to make a direct comparison between the severity of these two distinct types of storm event. The tornado modelled here is similar to that used by a previous worker [19] and has a maximum tangential velocity above the boundary layer of 90 m/s, a core radius of 60 m and a translational velocity of 20 m/s within an environmental wind which has a velocity of 20 m/s at a height of 10 m. The thickness of the boundary layer outside the tornado is 460 m and the thickness of the boundary layer within the tornado increases in an exponential and asymptotic manner from zero at the core to the external value at a large distance

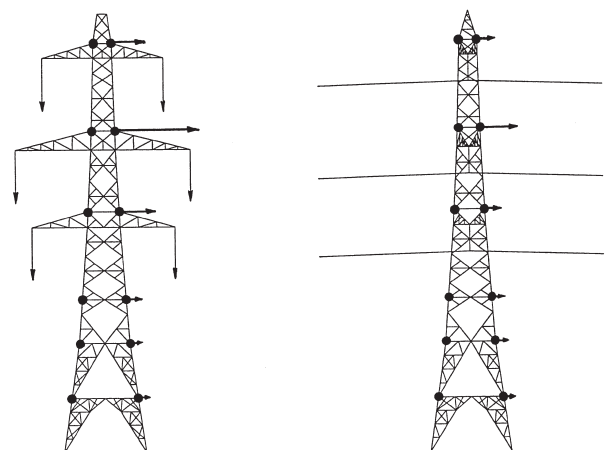


Fig. 5. Application of the wind loading to the tower.

from the tornado. This is illustrated by the dashed line in Fig. 1. The height of the boundary layer at any radial location within the tornado is defined by the point where the radial velocity becomes zero. The track of the event is such that the eye of the tornado passes at right angles across the transmission line at a distance of 50 m from the nearest tower. Hence, the upwind face of the tower is also normal to the tornado path. The configuration is illustrated in Fig. 6. It is recognised that, in many practical cases of tower failure, the axis of the tornado will be far from the vertical direction when it interacts with the tower, thereby inducing different loading distributions. In addition, the main tornado may have many smaller suction vortices which will also influence the loading. Nevertheless, for the initial study presented here only a single tornado with a vertical axis is investigated. The duration of the tornado interaction with the tower is very brief and so the time step for the tornado wind field prediction was taken to be 0.1 seconds (giving step intervals of 2 m for the horizontal translation of the tornado).

The modelled microburst is similar to that presented by other workers [23], which was based upon a real event. Although wind speeds of up to about 70 m/s have been recorded in microbursts it is evident that the maximum speeds may be somewhat higher in unrecorded events or in those where the recording instrumentation was damaged or destroyed. Hence, a maximum radial speed of 80 m/s is adopted for the present case. In addition, a translational speed for the event of 20 m/s has been chosen as being broadly representative of field

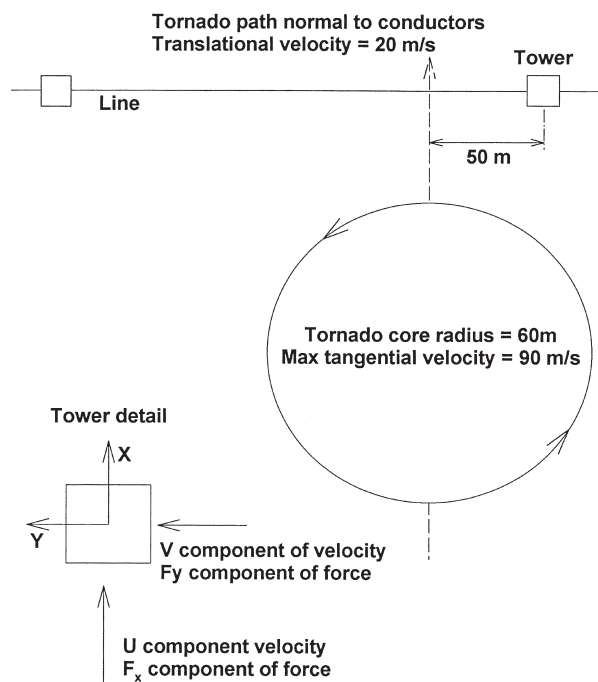


Fig. 6. Schematic of the modelled tornado characteristics and path relative to the tower.

data [23], as well as providing a degree of similarity with the modelled tornado. Since it has been noted [17] that a microburst may have an overall diameter of about 2 km (encompassing the whole downward “jet”), a core radius of 650 m has been used in the present case. This is effectively the distance from the core to a low barometric pressure ring within the microburst. From the analysis and field data of previous work [23] a characteristic radial length scale of 350 m has been adopted for the model in order to provide the correct shape for the radial velocity profile. This value is of the order of half the core radius and represents the distance outward from the core radius to where the high pressure ring occurs. The life time for a microburst may be as short as five minutes after touch down [17] and so, based on the assumption that after this time the radial velocity has reduced to 20% of its original maximum value, this gives a time scale of 200 seconds for the model. The radial length scale and the time scale are both inputs into the model equations [23] to give the microburst the correct radial velocity profile and decay rate (lifetime), as observed in nature. A reasonable value [17,22] for the height above the ground to the location of the maximum radial velocity in the microburst is about 60 m and this is used in the present calculations. The computations presented here are for a microburst which touches down some 1.5 km upstream of the transmission line and is then convected along a path which passes at right angles to the conductors such that the microburst centre passes at a distance of 100 m from the nearest tower. Hence, again, the windward face of the tower is normal to the path. The microburst event is of longer duration than that of the tornado and, therefore, one second interval time steps have been used in the calculations (giving step intervals of 20 m for the horizontal translation of the microburst). The microburst configuration is shown in Fig. 7.

6. Predicted wind fields and loads

The U and V horizontal components of the velocity time history for the tornado, occurring at a height above the ground corresponding to the centre of the top analysis region (section 1, shown in Fig. 4), are given in Fig. 8, together with the W vertical component. The computations commenced with the tornado located 1 km upwind of the tower and, after about 40 seconds, the tower begins to be influenced by the tangential component of the tornado, giving rise to an increase in the lateral (V) component wind speed. At about 48 seconds the V component reaches a peak and then decays to close to its original value by 50 seconds when the other two components reach their peaks. The U component achieves a maximum of about 115 m/s which is greatly in excess of that achieved in the microburst case, described

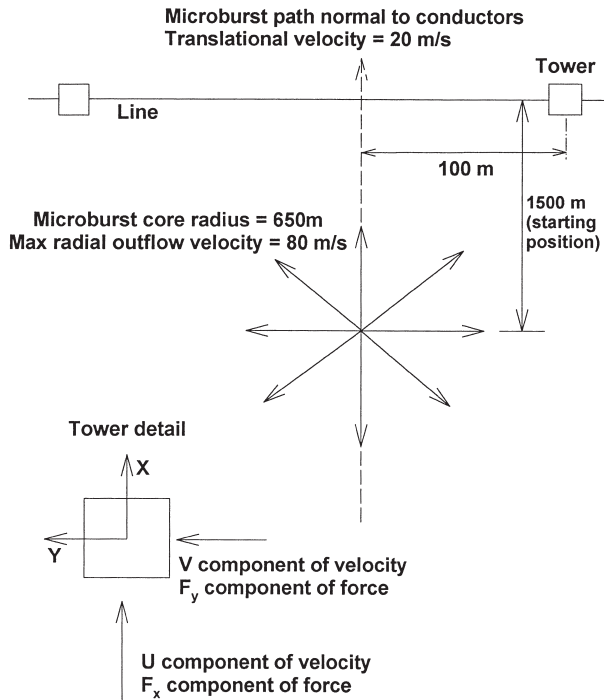


Fig. 7. Schematic of the modelled microburst characteristics and path relative to the tower.

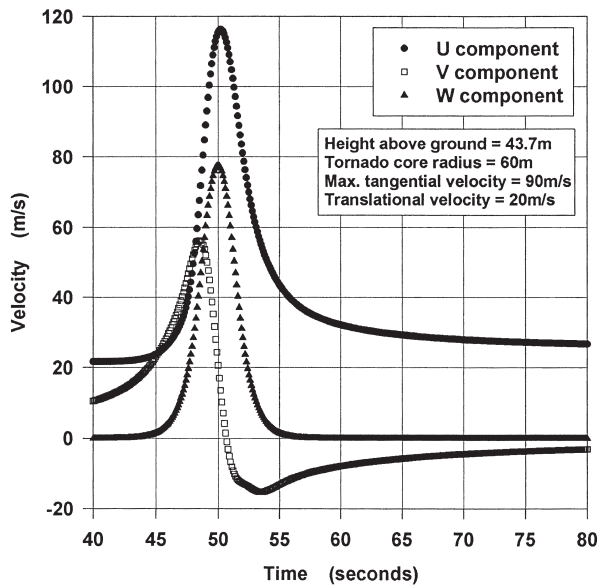


Fig. 8. Time history of the tornado wind speed components at centre of Section 1 of the tower.

below. The corresponding loadings on the highest section of the tower (section 1, Fig. 4), which includes the top pair of cross-arms, are given in Fig. 9. In this case both the normal and lateral loadings are significant, although the excess loads persist for only about 10 seconds with the normal direction force reaching a peak of about 240 kN.

The horizontal components of the velocity time his-

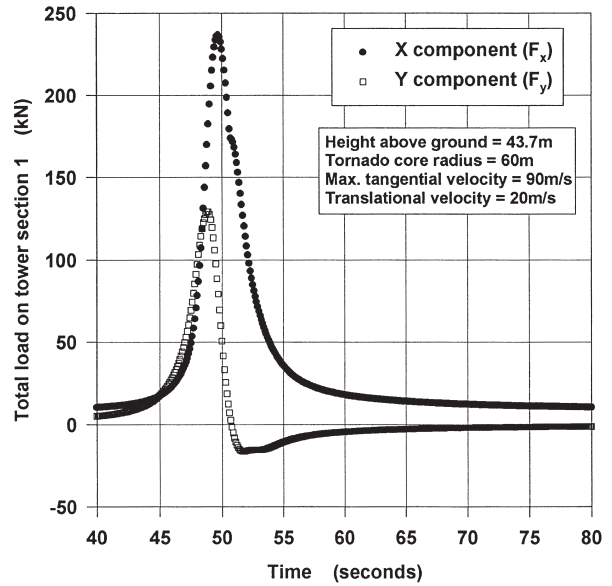


Fig. 9. Time history of the tornado horizontal wind loading components acting on Section 1 of the tower.

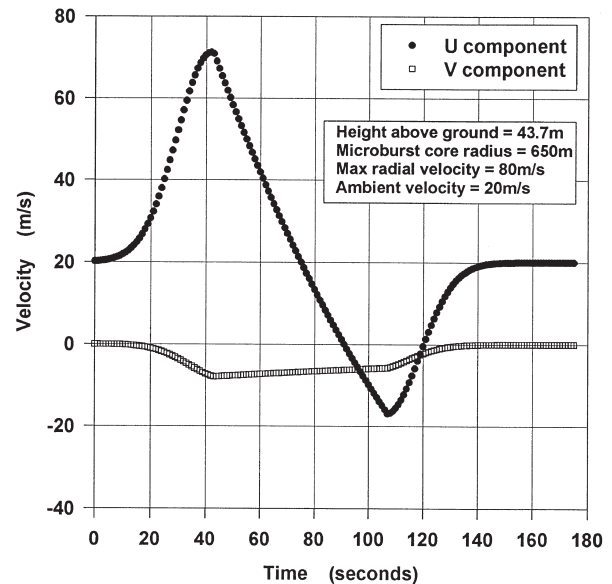


Fig. 10. Time history of the microburst horizontal wind speed components at the centre of Section 1 of the tower.

tory for the microburst, occurring at the centre of the highest “patch”, are shown in Fig. 10. These indicate that the effect of the decaying event as it passes the tower lasts for about 140 seconds. The lateral velocity component is rather weak but the normal component reaches a peak of about 70 m/s after about 40 seconds from the time of touch down. The corresponding total loading on the highest section of the tower, which, again, includes the top pair of cross-arms, is shown in Fig. 11. This indicates that a normal force on the tower, in excess of that due to ambient wind conditions in the absence

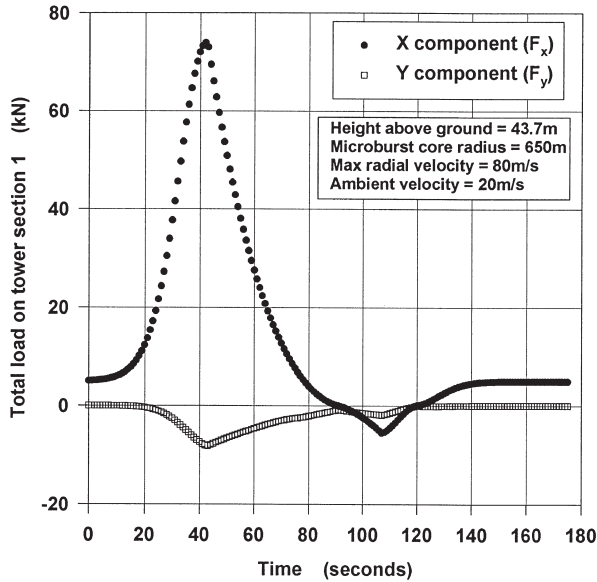


Fig. 11. Time history of the microburst horizontal wind loading components acting on Section 1 of the tower.

of the microburst, persists for about 60 seconds. This force varies with time and reaches a peak of about 75 kN.

The wind speed and loading time histories show very smooth profiles since, as mentioned earlier, other, smaller, scales associated with turbulent fluctuations have been neglected. It is necessary to note that these fluctuations, which may have frequencies closer to the natural frequencies of the structure (of the order of 2.2 Hz [29]), may also influence the response of the tower and, thereby, produce more critical results.

7. Response of the structure

The tower model has been examined under three different dynamic wind loads. The first of these is the tornado horizontal wind loading, whilst the second is the microburst wind load. In the third analysis 50% of the tornado load has been applied. The full tornado wind load creates unbounded responses signifying failure in the structure. In Fig. 12 the displacement time history at the top of the tower in the x -direction is shown, together with the time history of the total horizontal load in the x -direction. It can be seen that the structure shows an initial quasi-static response before becoming unbounded prior to the time of the peak load. The time history of the displacement at the top of the tower in the y -direction and the total horizontal load in the same direction are shown in Fig. 13. It can be seen from Fig. 12 Fig. 13 that when the displacement in the x -direction is becoming unbounded, the y -displacement remains in a bounded state. Hence, it is clear that the failure of the tower takes place in the x -direction.

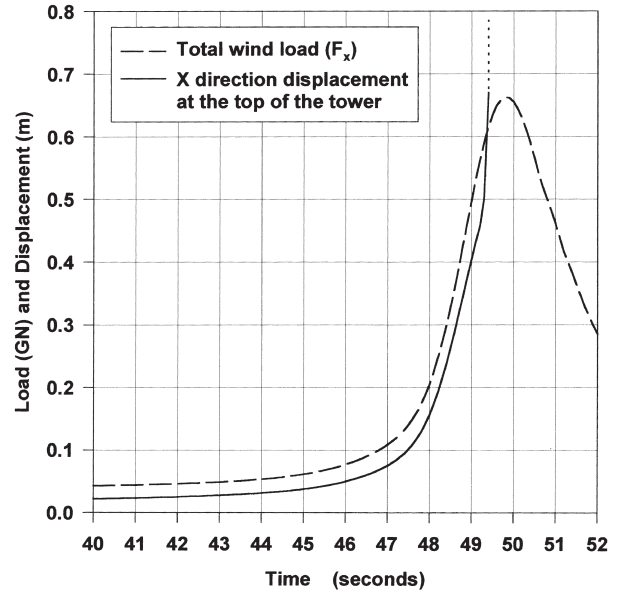


Fig. 12. Displacement of the top of the tower in the x -direction due to the tornado loading.

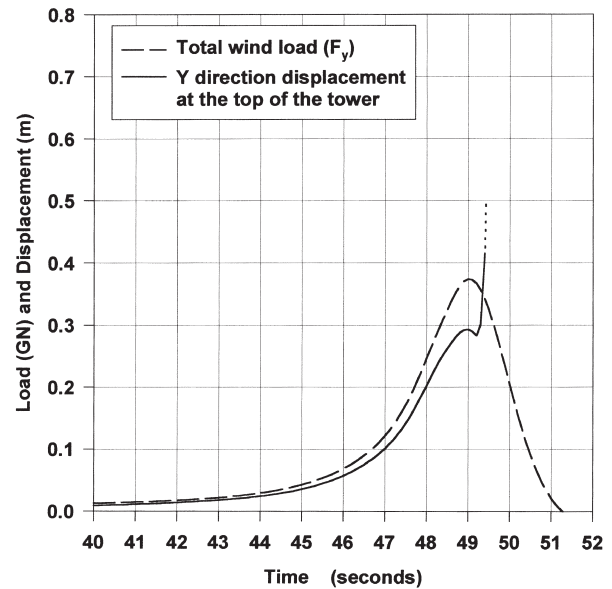


Fig. 13. Displacement of the top of the tower in the y -direction due to the tornado loading.

Two principal actions, namely overturning bending and horizontal shear, are produced in the structure by the horizontal wind loads. Examination of the post failure shapes of the structure reveals that the total horizontal shear force has caused failure in the structure. The failure occurs in a horizontal plan bracing section at the top of Section 5, as indicated in Figs. 14 and 15. The global shear force creates axial compression in some of the main members of this horizontal plan bracing. When this axial load exceeds the limit point load of the individual members, buckling takes place. As can be observed

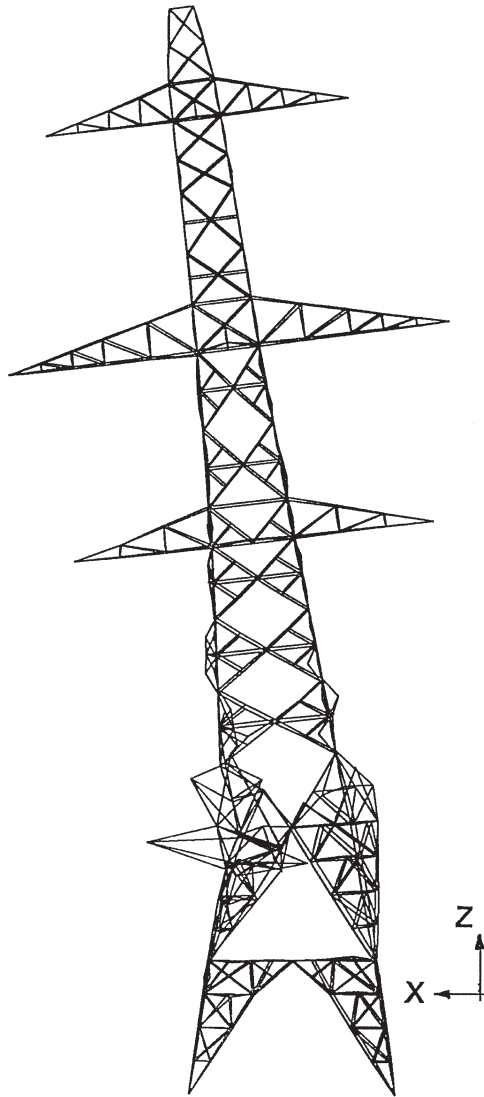


Fig. 14. Failure shape of the tower under the modelled tornado loading.

from the deformed shapes, at first one of the edge members in the x -direction of the plan bracing and on the leeward side of the tower, buckles. It can be seen that this buckling produces large horizontal deformation at the node in the middle of the member that is not restrained in the horizontal plane. After this, failure in the edge member in the x -direction occurs and the edge member in the y -direction on the leeward side of the tower also becomes unstable. Later, the interior members of the plan bracing fail in both the x and y directions. Failure of these bracing members produces large deformations at some horizontally unrestrained nodes. These deformations create successive buckling in other vertical and diagonal members. The last and, probably, critical failure occurs in the main tower leg, on the leeward side. This column carries a considerable compressive load and its instability creates a global collapse of the tower.

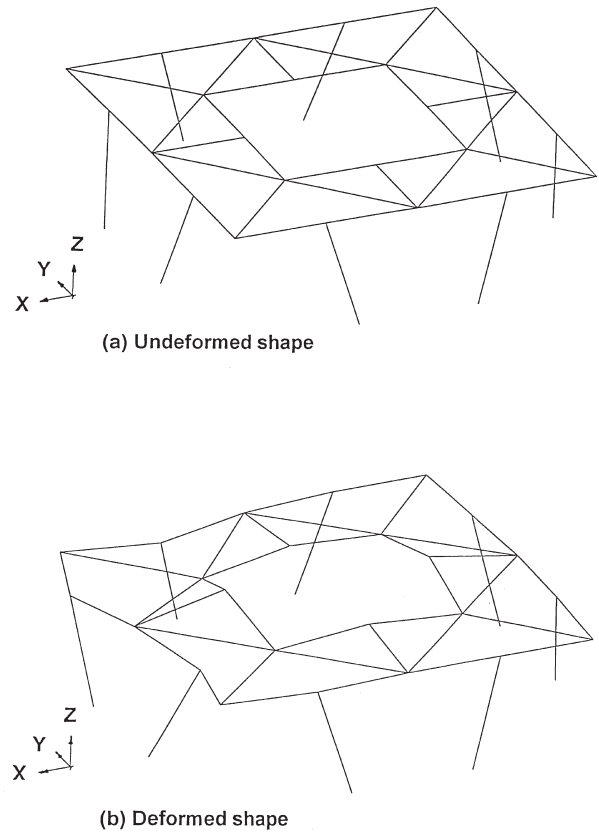


Fig. 15. Detail of the failure at the plan bracing between Sections 4 and 5.

The structural failure described above takes place in the second level of plan bracing in the tower above the ground (Section 5) and not at the first level (Section 6). The computations of the wind load show that the total horizontal shear force at the second level of the plan bracing (that is, the sum of the horizontal shear loads above this level) is almost the same as the horizontal shear applied at the first plan bracing section. However, the first horizontal plan bracing is considerably stiffer than the second one and so this makes the latter more vulnerable to failure produced by the wind-induced horizontal shear forces. In the higher levels of plan bracing there is a significant reduction in the applied horizontal shear force. The mode of failure outlined here appears to be in agreement with some of the field observations of collapsed towers [7] in which localised failure is followed by an overturning of the upper sections of the tower which generally remain undamaged by the wind.

As mentioned earlier, the response of the structure becomes bounded when the applied loads are lower than the minimum guaranteed critical load. When subjected to 50% of the tornado wind load, the load and deflection time histories at the top of the tower in the x and y -directions are as plotted in Figs. 16 and 17, respectively. Although high displacements can be seen in the response

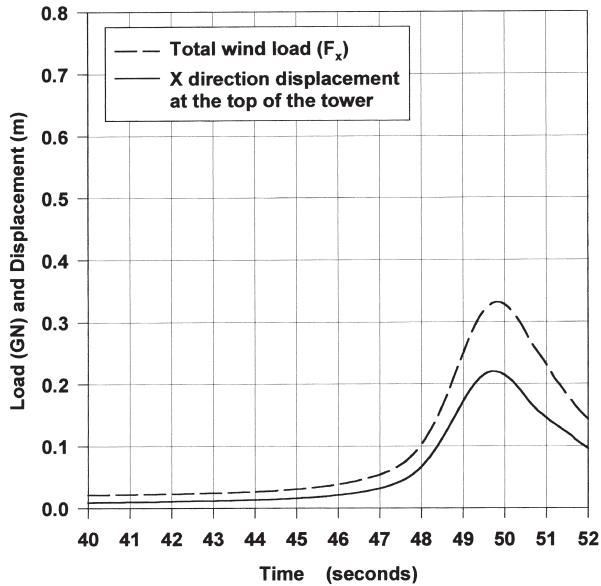


Fig. 16. Displacement of top of tower in the x -direction due to 50% of the tornado load.

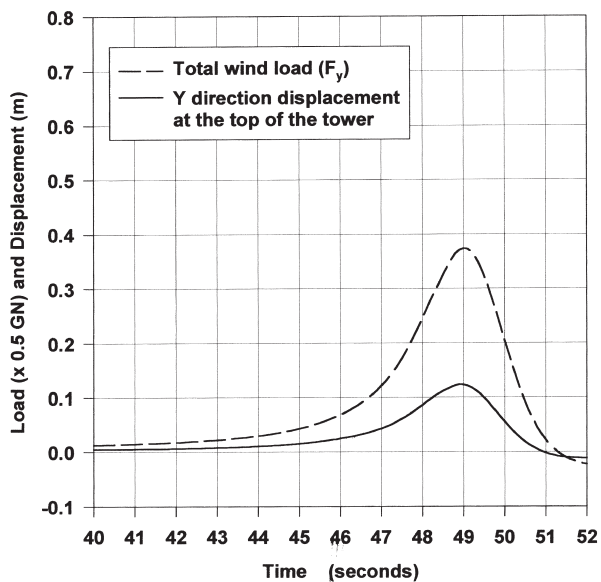


Fig. 17. Displacement of top of tower in the y -direction due to 50% of the tornado load.

close to the peak load, the displacements remain bounded at all times.

The response of the tower to a horizontal microburst wind load is shown in Fig. 18. It can be seen that the displacement reaches its maximum at the time of the maximum total load. The displacement remains proportional to the applied load throughout the time history and, hence, no significant non-linearity has occurred in the structure. Hence, a quasi-static response occurs with this kind of loading history, such that any failure associated with a microburst is more likely to be due to other influences. These may be either the additional effects of

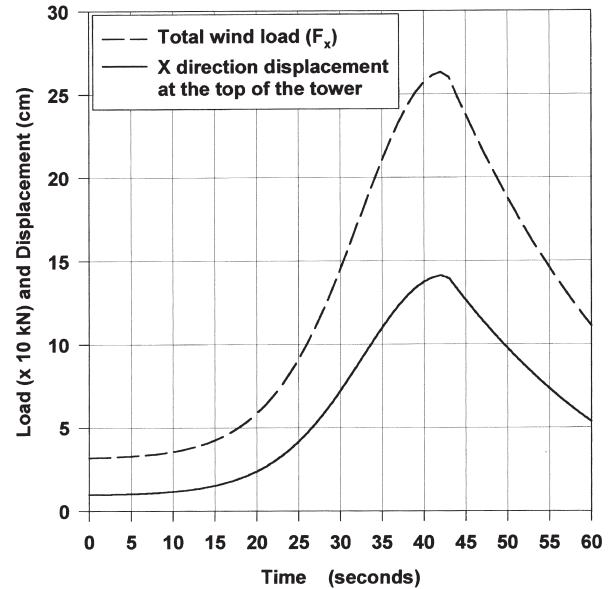


Fig. 18. Displacement of top of tower in the x -direction due to the microburst loading.

the smaller-scale fluctuations within the microburst structure, or the result of a broader-fronted, high-magnitude loading pattern that will include significant loading contributions from the conductors. However, these aspects remain the subject of further investigations.

8. Concluding remarks

The present work forms the starting point for a more detailed parametric study of the loading and response of transmission towers due to tornadoes and microbursts. In particular, it is intended to examine the effects of the scale and intensity of the HIW events and the path of the event relative to the tower. In addition, the influence of the conductor loads and the effects of HIW on other types of tower structure need to be studied, particularly guyed mast towers which are common in many areas where HIW events are a regular occurrence.

It is clear that both the wind loading models for the meteorological events and the subsequent structural analysis for the tower presented here contain many simplifications. Nevertheless, the results from the predictions are encouraging in that the tornado failure appears to concur well with evidence from the field, whilst the effect of the microburst is clearly less severe in the form modelled here. It is anticipated that the models and analysis used in this study will be refined during the course of further investigations.

Acknowledgements

The authors are indebted to the Engineering and Technology Division of The National Grid Company Plc,

United Kingdom, for supporting participation in the International Task Force Committee on HIW on Transmission Lines. In particular, thanks are due to Dr Roberto H Behncke (Senior Consultant — Overhead Lines) for his support and encouragement in this research area.

References

- [1] Engineering Sciences Data Unit (ESDU). Lattice structures Part 1: mean fluid forces on single and multiple plane frames. Wind Engineering Sub-Series, Data Item 81027, London, 1988.
- [2] Engineering Sciences Data Unit (ESDU). Lattice structures Part 2: mean fluid forces on tower-like space frames. Wind Engineering Sub-Series, Data Item 81028, London 1988.
- [3] International Electrotechnical Commission (IEC). Loading tests on overhead line towers. Report 60652, 1st ed., Technical Committee 11: Overhead Lines, 1979.
- [4] International Electrotechnical Commission (IEC). Loading and strength of overhead transmission lines. Report 60826 TR0, 2nd ed., Technical Committee 11: Overhead Lines, 1991.
- [5] American Society of Civil Engineers (ASCE). Guidelines for electrical transmission line structural loading. ASCE Manuals and Reports on Engineering Practice, No. 74, New York, 1991.
- [6] Loredou-Souza AM, Davenport AG. Wind tunnel modelling of transmission lines. In: Proc. 3rd Int. Coll. on Bluff Body Aerodynamics and Applications. Virginia, USA:Blacksburg, July 1996, Paper No B XI 9–B XI 12.
- [7] Dempsey D, White HB. Winds wreak havoc on lines. Transmission and Distribution World, June 1996:32–42.
- [8] Wen Y-K, Ang AHS. Tornado risk and wind effects on structures. In: Proc. 4th Int. Conf. on Wind Effects on Buildings and Structures, London, 1975:63–74.
- [9] Twisdale LA, Dunn WL. Wind loading risks from multivortex tornadoes. J Struct Engng, ASCE 1983;109:2016–22.
- [10] Milford RV, Goliger AM. Tornado risk model for transmission line design. J Wind Engng and Ind Aero 1997;72:469–78.
- [11] Lezaola J, de Schwarzkopf MLA, Rosso LC, Carstairs D. The influence of severe meteorological events on EHV conductor selection. Paper at University of Western Ontario Workshop on Control of Damage to Transmission Lines due to HIW, London, Ontario, Canada, October 1997.
- [12] Krishnasamy SG. Assessment of weather induced transmission line loads on a probabilistic basis. IEEE Trans Power App and Syst 1985;104:2510–6.
- [13] McMahon B. Reliability and maintenance practices for Australian and New Zealand HV transmission lines. In: Proc. 2nd Int. Conf. on Reliability of Transmission and Distribution Equipment, Coventry, UK, March 1995:198–203.
- [14] Oliver SE, Moriarty WW, Holmes JD. A severe thunderstorm risk model for transmission line design: Queensland and New South Wales. Australian Bureau of Meteorology Special Services Unit, ESAA Report No. 4, July 1996.
- [15] Holmes JD. Modelling of extreme thunderstorm winds for wind loading of structures and risk assessment. In: Larson A, Larose GL, Livesey FM, editors. Wind engineering into the 21st century. Rotterdam: Balkema, 1999:1409–15.
- [16] Fujita TT. Tornadoes and downbursts in the context of generalised planetary scales. J Atmospheric Sci 1981;38:1511–33.
- [17] Fujita TT. Downbursts: meteorological features and wind field characteristics. J Wind Engng and Ind Aero 1990;36:75–86.
- [18] Rinehart RE, Borho A, Curtiss C. Observations of microburst rotation. In: Proc. 26th Int. Conf. on Radar Meteorology, Norman, OK, USA, May 1993:676–678.
- [19] Wen Y-K. Dynamic tornadic wind loads on tall buildings. J Struct Div ASCE ST1 1975;101:169–85.
- [20] Zhu S, Etkin B. Model of the wind field in a downburst. J Aircraft 1985;22:595–601.
- [21] Ivan M. A ring–vortex downburst model for flight simulations. J Aircraft 1986;23:232–6.
- [22] Vicroy DD. Assessment of microburst models for downdraft estimation. J Aircraft 1992;29:1043–8.
- [23] Holmes JD, Oliver SE. A model of downburst winds near the ground for transmission line loading. CSIRO Div. of Building, Construction and Engineering, Australia. Report DBCE Doc 96/3 (M), January 1996.
- [24] Holmes JD, Oliver SE. An empirical model of a downburst. Engng Struct 2000;22(9):1167–72.
- [25] Letchford CW, Illidge G. Turbulence and topographic effects in simulated thunderstorm downdrafts by wind tunnel jet. In: Larson A, Larose GL, Livesey FM, editors. Wind engineering into the 21st century. Rotterdam: Balkema, 1999:1907–12.
- [26] Wood GS, Kwok KCS, Motteram NA, Fletcher DF. Physical and numerical modelling of thunderstorm downdraft. In: Larson A, Larose GL, Livesey FM, editors. Wind engineering into the 21st century. Rotterdam: Balkema, 1999:1919–24.
- [27] Lomas C. Transmission tower development in the UK. Engng Struct 1993;15(4):277–88.
- [28] ABAQUS. ABAQUS Version 5.7. Providence, Rhode Island, USA: Hibbitt, Karlsson and Sorensen Inc, 1998.
- [29] Savory E, Parke GAR, Disney P, Toy N, Zeinoddini M. Field measurements of wind-induced transmission tower foundation loads. J Wind and Struct 1998;1:183–98.
- [30] ECCS. Recommendations for angles in lattice transmission towers, European Convention For Constructional Steelwork. Technical Committee 8 — Structural Stability, Technical Working Group 8.1 — Components, Report No. 39, 1985.
- [31] British Standards. Lattice towers and masts. Codes of Practice for Loading, BS 8100: Part 1, London, 1986.
- [32] Scruton C. An introduction to wind effects on structures, Engineering Design Guide No. 40. UK: Oxford University Press, 1981.
- [33] Fujita TT. Experimental classification of tornadoes in FPP scale. SMRP Research Paper 98, Univ. of Chicago, USA, 1973.